Biochemical Engineering Journal 105 (2016) 150–158

Contents lists available at ScienceDirect

Biochemical Engineering Journal

journal homepage: www.elsevier.com/locate/bej

Regular article

Kinetics of *Pseudomonas veronii* 2E biofilm development under different nutritional conditions for a proper bioreactor design

María Alejandra Daniel[a], Matías R. Barrionuevo[a], Santiago R. Doyle[b], Diana L. Vullo[a,*]

[a] *Área Química, Instituto de Ciencias, Universidad Nacional de General Sarmiento-CONICET, J.M. Gutiérrez 1150, (B1613GSX) Los Polvorines, Buenos Aires, Argentina*

[b] *Área de Biología y Bioinformática, Instituto de Ciencias, Universidad Nacional de General Sarmiento, J.M. Gutiérrez 1150, (B1613GSX) Los Polvorines, Buenos Aires, Argentina*

ARTICLE INFO

Article history:
Received 6 March 2015
Received in revised form 20 August 2015
Accepted 2 September 2015
Available online 9 September 2015

Keywords:
Wastewater biotreatment
Metal bioremediation
Biofilm reactor
Pseudomonas veronii
Biofilm stability
Biosorption

ABSTRACT

Biofilm-mediated bioreactors represent a proficient alternative, as extracellular materials of bacterial biofilms enhance metal immobilization by biosorption. Bacterial attachment or detachment is related to environmental conditions. The aim of this work is to study the nutritional dependence of *Pseudomonas veronii* 2E biofilm development to be applied in a future biofilm-reactor for wastewater treatments. For such purpose, biofilm establishment kinetics was explored over glass coverslips changing medium composition and nutrient concentration and in Fe(II) presence. After crystal violet cell staining, biofilm was visualized using direct microscopic observation; sample scanning-image analysis implemented in MATLAB and ethanol extraction-Absorbance 590 nm measurement. Biofilm structure developed with mineral basal medium appeared as a monolayer, but in complex basal media cell aggregates were appreciated. Optimal attachment was achieved with complex basal medium-5 g/L glucose at 55 h. The crystal violet concentration complemented with the image capturing supported these results. Biofilm establishment was enhanced by biosurfactant production in *P. veronii* 2E. The obtention of mutants deficient in biosurfactant secretion confirmed the influence of these compounds on cell motility and hence on cell attachment. The information of the biofilm structure defined under such conditions is the useful first step for the future bioreactor design.

1. Introduction

Biofilms are surface-associated microbial communities where microorganisms form flocks and aggregates. They are found in every moist environment where a nutrient flow is available and surface attachment can be achieved. Microorganisms are embedded in a biofilm matrix, formed by extracellular polymeric substances (EPS) produced by themselves.

Industrial effluent biotreatments mediated by biofilms present a more proficient and safer alternative than those performed with planktonic microorganisms. Cells are protected within the matrix, leading to their adaptation and better survival from the potential toxicity of wastewaters. Biofilms support a high biomass density maintaining optimal conditions of pH, localized solute concentrations and redox potential in cell surroundings. The secreted polymers that form the matrix have the ability to immobilize several chemical species by biosorption or biomineralization, together with the bioaccumulation processes, performed by microbes [1]. These mechanisms are of particular interest in metal bioremediation. Most spread biofilm reactors in wastewater treatments are upflow sludge blanket reactors (USBR), packed/fluidized bed reactors (P/FBR) and airlift reactors (ALR) [2].

As proved for *Pseudomonas aeruginosa*, biofilm development and establishment, as well as its dispersion, can be induced by the physicochemical or nutritional conditions of the environment [3,4]. Temperature, carbon or nitrogen source nature and concentration, presence or absence of Fe(II) are example parameters of relevance for biofilm stability in time. Regarding bioreactor performance, biofilm maintenance is an important feature to keep, making a bioremediation process successful. Though changes in biofilm evolution can be studied by applying the traditional crystal violet dying method [5,6] and for specific biofilm structural analyses atomic force microscopy, confocal laser scanning microscopy,

Abbreviations: OD, optical density; CV, crystal violet; FD, fractal dimension; 3D, three dimensional; ST, surface tension; NH_2-, amino.

* Corresponding author. Fax: +54 1144697501.
E-mail addresses: mdaniel@ungs.edu.ar (M.A. Daniel), matxfiles@hotmail.com (M.R. Barrionuevo), sdoyle@ungs.edu.ar (S.R. Doyle), dvullo@ungs.edu.ar (D.L. Vullo).

http://dx.doi.org/10.1016/j.bej.2015.09.001
1369-703X/

scanning electron microscopy [2], a simpler and accessible technique is applied by capturing biofilm images in conjunction with their analyses by an adequate software [7].

The aim of this work is to study biofilm development of *Pseudomonas veronii* 2E over glass, varying nutritional parameters in order to optimize biofilm establishment and maintenance as a first step for further utilization in packed or fluidized bed reactors to be applied in metal loaded wastewater treatments, particularly for Cd(II) and Zn(II) biosorption. An innovative way of biofilm structural analyses is presented by image capture by scanning and image processing implemented in MATLAB.

2. Materials and methods

2.1. Microorganism

P. veronii 2E was isolated from polluted surface waters (Reconquista River, Buenos Aires Metropolitan Area) and identified both by biochemical and molecular methods as previously described [8]. This microorganism demonstrated maximal adsorption capacity toward Cd(II) and Zn(II) at 32 °C, pH 7.5 and ability to develop biofilms on different polymeric matrices. These metal–cell interactions were reported in previous works and demonstrated to be restricted to a physicochemical mechanism on the cell surface [8,9].

2.2. Biofilm development studies

2.2.1. Inocula preparation

P. veronii 2E was grown in 10 mL of any culture broth and after 72 h at 32 °C and 120 rpm, 2 mL were transferred to 20 mL of the same medium. The bacterial cultures obtained after 24 h at 32 °C and 120 rpm were used as inocula for biofilm formation assays.

2.2.2. Culture media

Several types of basal culture media, a minimal saline medium M9 (g/L: 7.3 K_2HPO_4; 3.0 KH_2PO_4; 1.0 NH_4Cl; 0.5 NaCl; 0.246 $MgSO_4{\cdot}7H_2O$; 0.01 $CaCl_2$) and three complex media: a) PcY (g/L: 2.5 casein peptone; 1.25 yeast extract), b) PY-N_{Amino} (g/L: 2.27 meat peptone; 1.25 yeast extract) and c) PY-N_{Total} (g/L: 2.5 meat peptone; 1.25 yeast extract) were used for testing the influence of nutritional parameters on biofilm establishment.

As carbon sources, glucose, sodium citrate, sodium glutamate and sodium succinate were added separately to a final concentration of 5 g/L or 10 g/L when using M9 or PcY. PY-Complex media were chosen based on the variation of N content and nature of the protein hydrolysates, so they were supplemented only with 0.5 or 5 g/L glucose.

For testing Fe(II) influence on biofilm establishment, final 3 μM was added to M9 or PcY media.

2.2.3. Immobilization matrix

Glass coverslips (18 mm × 18 mm, thickness N°1 0.13–0.16 mm, borosilicate D 263™ of the first hydrolytic class, chemically resistant, Marienfeld) were chosen as material for bacterial fixation and biofilm development. A 2 h-washing procedure with alkaline tensoactive together with a rinse with distilled water were carried out before autoclaving, required as an adequate surface preparation.

2.2.4. Biofilm development kinetics

Kinetics of biofilm formation was evaluated in static conditions at 32 °C and with the following culture media: M9-glucose, M9-sodium citrate, M9-sodium glutamate, M9-sodium succinate, M9-Fe-glucose, PcY-glucose, PcY-Fe-glucose, PcY-sodium citrate, PcY-sodium glutamate, PcY-sodium succinate, PY-N_{Amino}-glucose, PY-N_{Total}-glucose. In all cases a coverslip was introduced in each well of 6-well polystyrene microplates, before adding 3 mL of a bacterial suspension, previously prepared mixing 45 mL fresh medium with 5 mL of the bacterial culture. Incubation was performed at the chosen temperature and observations on biofilm development were registered at 0 h (t_0), 7 h (t_1), 31 h (t_2) and 55 h (t_3) with a washing step and medium renewal at 30 h. Planktonic growth was controlled by Optical Density (OD) measurements at 600 nm and pH values were registered at any time.

Each incubation time was tested by triplicate and a cell-free control well was checked at t_0.

Coverslips were picked up at the different incubation times and washed with distilled water to eliminate free cells. Adhered cells were fixed to glass with a 7.2 w/v% formaldehyde solution for 30 min and, after washing again with distilled water, coveslips were exposed to a 1 w/v% crystal violet (CV) solution for 10 min for specific cell staining. Then, the dye excess was eliminated by rinsing twice with distilled water and a last third rinse was carried out by submerging the glass directly on distilled water. Finally, a drying step was performed at 32 °C.

For estimating cell concentration in biofilm mass during time, each coverslip was treated with 2 mL of ethanol 30 min at 150 rpm, 26 °C for CV dissolution. Absorbance at 590 nm of the ethanol extracts was measured and CV concentration was determined, which is proportional to adhered biomass as reported by other authors [6]. In parallel, one coverslip from the triplicates was observed under optical microscope Nikon Eclipse E200, registering the images with a Canon Power Shot G9 camera with 400× magnification.

2.2.5. Image acquisition

Before CV extraction, high resolution digital images of each coverslip were obtained with the aid of a flatbed digital scanner (Canon 5600f, Canon Inc.). Each image consisted on several plates, separated by a non-transmitting black surface. Since biofilm samples were obtained by culturing onto a thin glass support, images were obtained by transillumination, thus the digital levels of the pixels consisted on transmitted light. Images were acquired with a 4800 dpi resolution scanner setting. Actual spatial resolution of images was somehow half of its nominal value when experimentally estimated by scanning a microscope stage micrometer, being ~2400 dpi, equivalent to a 10.6 μm resolution. Color depth was set to 48 bit per pixel in order to achieve a high intensity resolution, and images were stored in a lossless format (TIFF).

2.2.6. Automated image analysis program

An image processing program aimed to perform in a completely automated fashion was developed in MATLAB (MATLAB r2009b, The Mathworks Inc.). The program has 3 main modules that will be briefly described below: 1) segmentation, which consists on locating each sample on the whole image, 2) estimation of biofilm abundance on each pixel of each sample, and 3) characterization of the biofilm spatial distribution. The solely inputs of the program are a set of digital images, each with several samples as previously described, and a Microsoft Excel® spreadsheet containing sample data. The spreadsheet contains an ID for each scanned sample, the name of the image file where the sample was scanned, and the row and column where the sample was placed in the image acquisition device, which allows to relate the sample ID with a portion of the whole scanned image.

For locating each sample on each scanned digital image, a technique called segmentation [10] was achieved. At first a fixed gray intensity threshold was applied to obtain a binary image, then connected areas were determined to obtain the image area corresponding to each sample on the images using built-in MATLAB functions [11]. The correspondence between each sample listed in the input data and a portion of the digital image was completed by

comparing the relative location of the center of each located sample with the location indicated by the user in the spreadsheet. The described procedure had the advantage of being robust to slight variations in the orientation when placing the image acquisition device on the scanner.

The second module of the automated program next analyzed each sample to estimate the mean abundance of biofilm on each sample, as well as at the pixel level. Since the mean digital level of each pixel is proportional to the mean transmitted light through the area of the sample, it was used to estimate dye abundance. This is possible given that the only pigment present on the image was the CV used to dye the sample. Biofilm abundance was estimated from mean digital levels in accordance to Lambert–Beer law:

$$-\log\left(\frac{T}{T_0}\right) = \epsilon c l \quad (1)$$

where T and T_0 are transmitted light and incident light respectively, and in the digital images have units of digital levels; ϵ is the absortivity constant; c is the concentration of the dye; and l is the length of light path through the sample, which in this case equals height of the biofilm. At the pixel level, Eq. (1) takes the form of:

$$\left(-\log T_{ij} + \log T_0\right) = \epsilon c l_{ij} \quad (2)$$

where the subindex ij indicates the pixel with row i and column j of the sample image, assuming that the concentration of dye is constant among the whole sample. The total amount of dye (d_{ij}) in the area of a pixel equation (s) is equal to:

$$d_{ij} = c s l_{ij} \quad (3)$$

Combining Eq. (2) and (3) and results in:

$$d_{ij} = (s/\epsilon)\left(-\log T_{ij} + \log T_0\right) \quad (4)$$

Eq. (4) allows estimating the value of the constant ϵ by relating the digital levels of all the pixels on an image with the total amount of dye in the sample (D_T) experimentally determined by classical spectrophotometry:

$$D_T = (s/\epsilon)\Sigma_i \Sigma_j \left(-\log T_{ij} + \log T_0\right) \quad (5)$$

where $i = 1, ..., n$ and $j = i, ..., k$ are the number of rows and columns of the image. Having the value of the constant ϵ, the amount of dye in each pixel can be easily estimated using Eq. (4), thus generating a map of the spatial distribution of the biofilm of each sample.

The third part of the developed program analyzed the spatial distribution of the biofilm. Characterizing spatial patterns can be complex, especially when dealing with continuous values like the biofilm spatial distribution rather that presence/absence data [12]. For the characterization of the biofilm spatial distribution, the fractal dimension (FD) was chosen for it is a metric that has been extensively used to characterize spatial patterns [13]. The FD has the advantage of synthesizing in a single value a geometrical property well suited to describe spatial patterns originated by organisms and other phenomena which are characterized by self-similar, scale-free behavior [14]. The spatial pattern of the biofilm was considered as a three-dimensional (3D) surface, where the z-axis is the amount of dye present on each pixel of the image. Furthermore, the 3D surface obtained as previously described is in turn proportional to the actual height of the biofilm in each pixel of the image if the concentration of dye is constant, due to Eq. (3). For such 3D surface, the FD can take a value between 2 and 3; FD would take values near 2 for smooth surfaces, such as a smooth paper, and would approach its maximum value of 3 if the surface increases in complexity and tends to "fill" the space, like a wrinkled paper. The FD was estimated by the box-counting method [14], which was implemented in MATLAB.

2.3. Biosurfactant production and influence on biofilm development

2.3.1. Detection of biosurfactant secretion

Biosurfactant production was evaluated by growing tested bacteria in two different media: Blue Agar (per L: $(NH_4)_2HPO_4$ 1.5 g, KH_2PO_4 4 g, Yeast Extract 0.4 g, *N*-cetyl-*N*,*N*,*N*-trimethylammonium bromide 0.2 g, Agar 15 g, add after autoclaving 1 M $MgSO_4$ 8 mL and 0.001 g/mL Methylen Blue 15 mL) and Blood Agar (per L: Meat Extract 3 g, Meat Peptone 5 g, Agar 15 g, add after autoclaving sheep blood 50–80 mL). Blue Agar assay was positive for anionic biosurfactants secretion by the visualization of a dark blue precipitation halo around the colonies after 48 h at 32 °C and 24 h of storage of grown plates at 4 °C. Meanwhile a haemolysis halo around colonies in Blood Agar after 24, 32 or 48 h at 32 °C was considered positive for any biosurfactant production.

2.3.2. Obtention of mutants deficient in biosurfactant production

P. veronii 2E was grown in the conventional Nutrient Broth supplemented with 10 mg/mL chloramphenicol and the mutagenic strain *Escherichia coli* S171 λpir/put TC in the same medium but supplemented with 10 μg/mL tetracycline and 100 μg/mL ampicillin, both at 32 °C up to an $OD_{600\,nm}$ = 0.9. Then, 0.2 mL of *P. veronii* 2E culture was mixed with 0.8 mL of *E. coli* S171 λpir/put TC culture. The mixture was centrifuged at 12,850 × *g* and after washing twice with 150 mM NaCl, cells were suspended in 20 μL of the same solution. The whole volume of the bacterial suspension was transferred to a cellulose acetate membrane of 0.22 μm pore diameter, located in a Petri dish with Plate Count Agar (PCA: casein peptone 5 g/L, yeast extract 2.5 g/L, glucose 1 g/L, agar 14 g/L). After an incubation of 7 h at 32 °C, the membrane was submerged in 1 mL of 150 mM NaCl and samples of 100 μL of the new suspension were spread on Blue Agar supplemented with 10 μg/mL tetracycline and 10 μg/mL chloramphenicol. Plates were incubated 5 days at 32 °C and non-producing mutants (MUT) were selected by the absence of both blue color and precipitation halo.

2.3.3. Surface Tension measurements

Surface Tension (ST) decrease in culture supernatants is an index of biosurfactant production mediated by microorganisms. *P. veronii* 2E or 2E MUT were grown by duplicates in a minimal basal medium (g/L: $(NH_4)_2HPO_4$ 1.5, KH_2PO_4 4, Yeast Extract 0.4, $MgSO_4.7H_2O$ 1.97) supplemented with 20 g/L glucose or 5 v/v% sunflower oil. After 1 month at 32 °C and 120 rpm, cultures were centrifuged at 6300 × *g*, 15 min. Supernatants were recovered and their corresponding STs were measured in dyne/cm by using a stalagmometer. ST can be calculated as the mean value of 10 determinations of:

$$ST = 72.75 WD\delta_{sol}/SD$$

where WD is the number of pure water drops, SD is the number of the solution drops that fall from the first to the last mark of the stalagmometer and δ_{sol} is the density of the solution.

This protocol was also performed with *P. aeruginosa* PA01 as reference strain.

2.3.4. Rapid biofilm formation test in 96-well microtiter plates

Overnight cultures of *P. veronii* 2E and the mutant 2E MUT were diluted (1:100) with M9 supplemented with 10 g/L glucose or 5 g/L sodium glutamate. Ten wells were filled with 100 μL of *P. veronii* 2E-M9-glucose dilution, ten with *P. veronii* 2E-M9-glutamate dilution, ten with 2E MUT-M9-glucose dilution and ten with 2E MUT-M9-glutamate dilution. After 24 h at 32 °C, the supernatants were discarded and then the biofilms were washed three times with 150 mM NaCl. Cells were fixed with 0.5 w/v% % formaldehyde and after washing with distilled water, 300 μL of 0.4 w/v% CV were

added and kept 20 min in contact at 26 °C and washed. Finally, CV was extracted with 200 μL ethanol and Absorbance at 590 nm was measured in each 1:4 dilution of the obtained extracts.

2.3.5. Swimming and swarming motility tests

These two types of motility were tested as previously described [15]. Swimming assays were carried out in duplicates in 10 mL-tubes containing 3 mL of PcY-5 g/L glucose medium. Swarming assays were performed in duplicates in Petri dishes (5 cm diameter), with a swarming agar formulation based on Nutrient Broth composition (Merck) supplemented with 5 g/L glucose, 3 g/L casein peptone and 0.04 g/L agar to increase medium viscosity. When necessary, 50 mg/mL of the synthetic surfactant Triton X-100 was added.

3. Results and discussion

3.1. Influence of the basal medium composition and carbon source effect on biofilm formation

The biofilm formation kinetics was evaluated using two different basal media: the minimal saline medium M9 and the complex medium PcY. In addition, glucose, sodium glutamate, succinate and citrate were tested in each medium as different carbon sources. Fig. 1a shows the obtained results on biofilm establishment

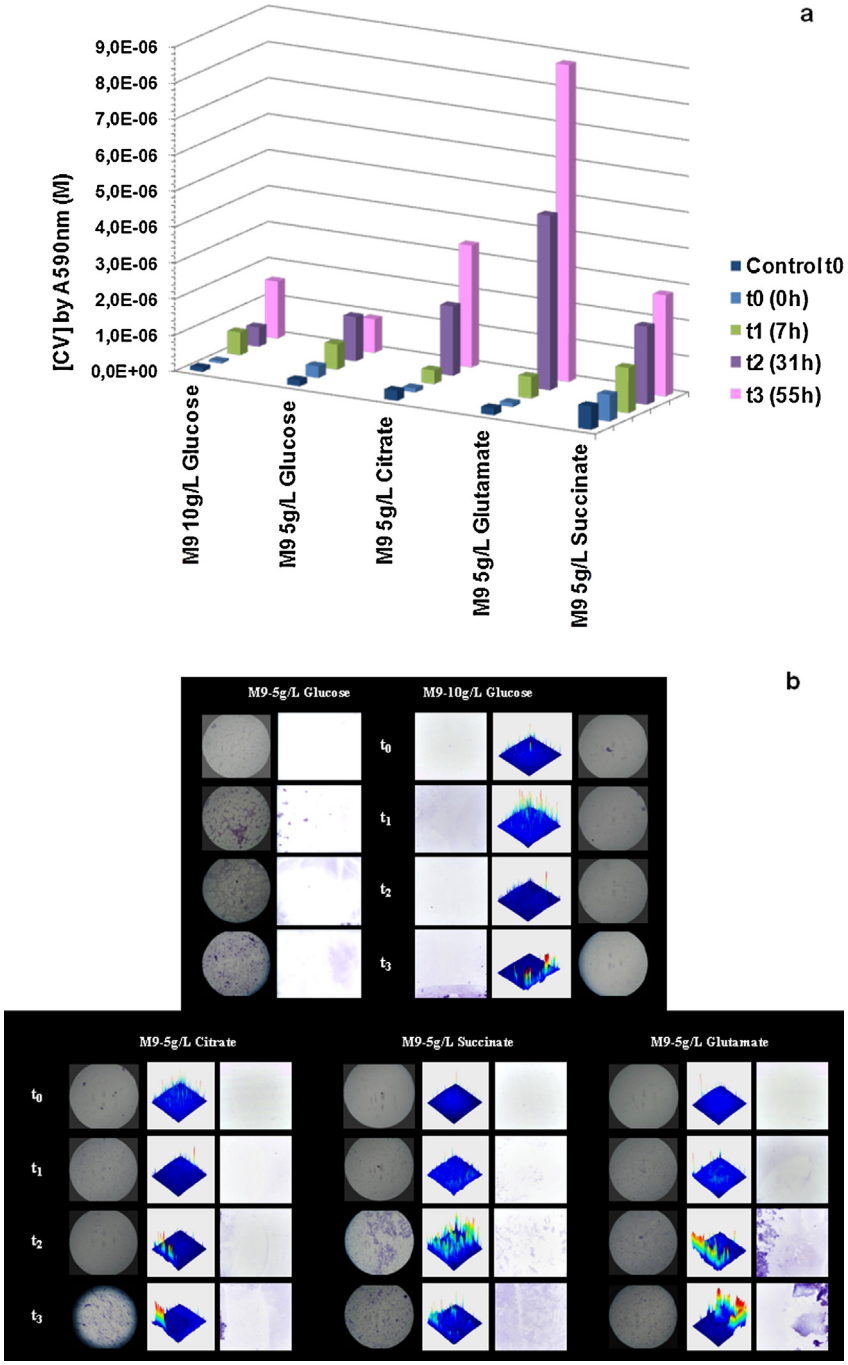

Fig. 1. Kinetics of biofilm formation in M9 basal medium in presence of different carbon sources evaluated by two methods: (a) CV assay and (b) image capturing and 3D-pattern development (t_0 = 0 h, t_1 = 7 h, t_2 = 31 h and t_3 = 55 h).

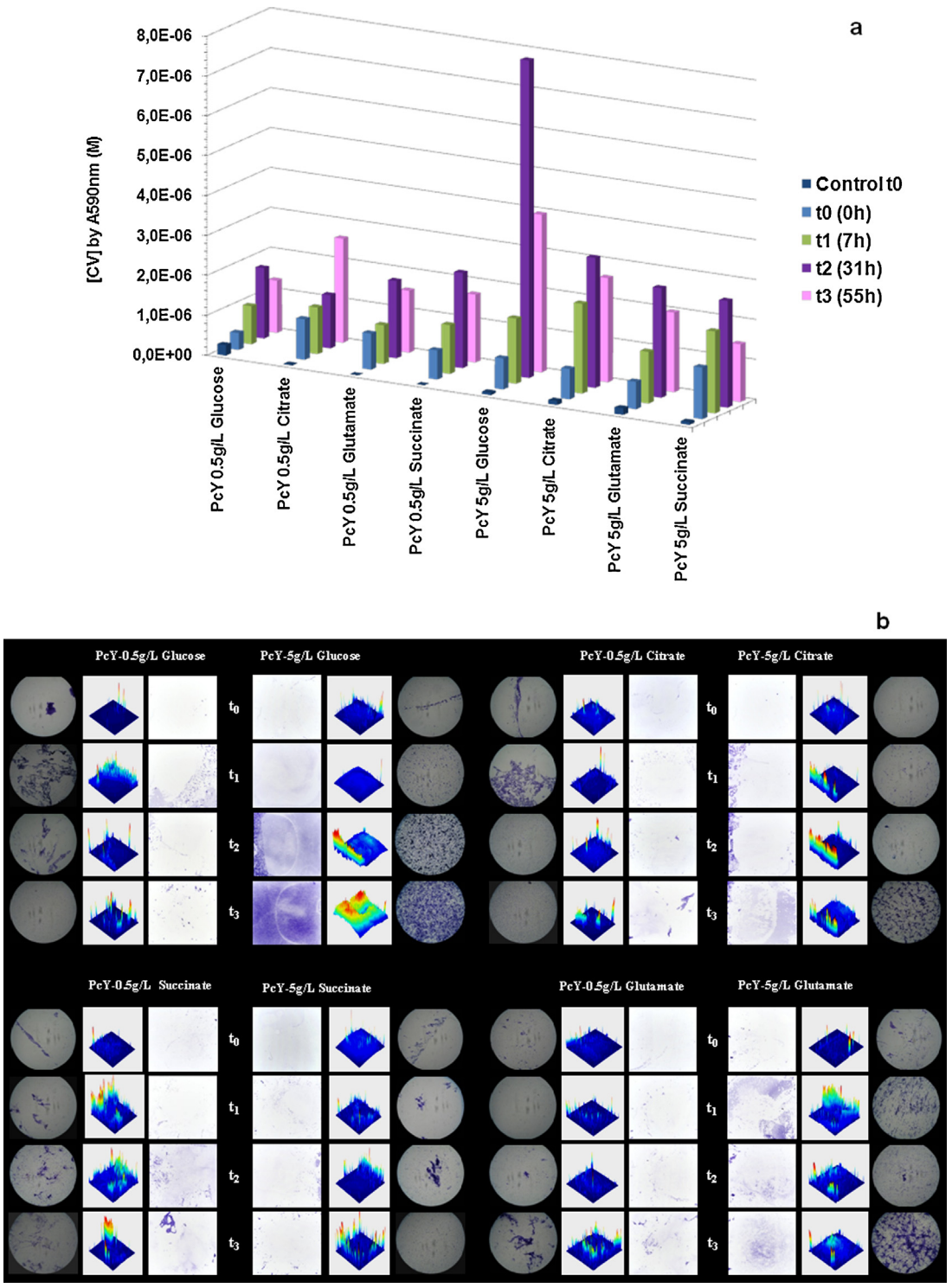

Fig. 2. Kinetics of biofilm formation in complex (PcY) medium in presence of different carbon sources evaluated by two methods: (a) CV assay and (b) image capturing and 3D-pattern development (t_0 = 0 h, t_1 = 7 h, t_2 = 31 h and t_3 = 55 h).

evolution in time in M9 basal medium, determined by the classical CV dying method. Implementing this procedure, the best attachment yields were achieved with M9-5 g/L sodium glutamate, being the maximal at 55 h (t_3). In contrast, Fig. 1b details the captured images during the same experience, revealing that the most homogenous biofilm was obtained with M9-5 g/L sodium succinate at 55 h. Highest levels of biofilm heterogeneity could be observed in both the scanned coverslips and the 3D surface pattern with M9-5 g/L sodium glutamate, either at 31 h (t_2) or 55 h (t_3). In consequence, the higher CV concentration obtained did not mean an uniform bacterial attachment. Thus, results were being masked when only CV measurements were performed as biofilm formation index. With M9-5 g/L sodium succinate, biofilm developed homogeneously, covering efficiently the whole glass surface.

Results obtained with the complex medium PcY are exposed in Fig. 2. Fig. 2a shows that, using the CV method, the best biofilm formation yields were registered with PcY-5 g/L glucose, with a maximum value at 31 h. In this case, the captured images were

mostly in agreement with the results, except for the heterogeneity of the obtained biofilms: at 55 h the more efficient and homogeneous coverage was achieved. A point to be considered is the correct interpretation of the results obtained by the integration between both techniques. For example, as seen with PcY-5 g/L glucose, at t_2 = 31 h an anomaly that should be taken into account was found. The CV concentration was the highest due to an irregular biofilm formation in the coverslip border (see Fig. 2b), consequence of an extra bacterial colonization over the available polystyrene of the well. This bacterial agglomeration increased the CV concentration, but it is not representative of the whole glass surface coverage as revealed the images and the 3D patterns. So, this fact should not contribute to a wrong conclusion of the biofilm formation kinetics in terms of confirming a cell detachment after 31 h, which would be inconsistent with the global analysis of the results.

The concentration effect of the carbon source is clear, since with 0.5 g/L only a thin biofilm was formed, independently of the tested compound. When PcY medium was used, a different biofilm profile was detected by microscopic observation. A large distribution of cellular aggregates were observed on the analyzed surfaces resembling the typical mushroom-like formations, while with M9 medium, a monolayer-like (flat) biofilm was mostly registered (compare Fig. 1b with Fig. 2b). Another additional data that can be extracted from Figs. 1 and 2 is that using both basal media no biofilm detachment was detected after medium renewal and up to the 55 h of study.

The dependence of biofilm formation with carbon source nature was studied for *P. aeruginosa* by other authors [16]. Clearly in mineral basal media, glucose promoted the development of structured biofilms with cell aggregates, while citrate gave flat and uniform biofilms. Both effects are related to cell motility (mediated by type IV pili or flagella), rhamnolipid production and *quorum sensing* [3]. Comparing in this aspect, *P. veronii* 2E biofilms were poorly developed with M9 as basal medium, and similarly small aggregates were observed only when glucose was the carbon source (Fig. 1b). *P. veronii* 2E is a biosurfactant producer [17], as revealed by several assays like the precipitation halo in Blue Agar and the haemolysis halo in Blood Agar (Fig. 3a). The confirmation of a surface tension decrease in culture supernatants, stimulated when a hydrophobic substrate was present, supports these results (Table 1). The obtention of a deficient producer mutant *P. veronii* 2E MUT was a preliminary result that evidenced the relationship between surfactant production and biofilm development in *P. veronii* 2E (see absence of characteristic halos in Fig. 3a and ST values in Table 1). This strain inefficiently produced biofilms, as analyzed with the rapid microtiter plate-CV technique which results are exposed in Fig. 3b. Interestingly, the swimming motility of the mutant strain was not altered showing that flagella activity was apparently normal. By contrast, its swarming motility was totally diminished (Fig. 4), being absolutely related to the decrease in biosurfactant

Table 1
Surface Tension (ST) values of culture supernatants of *P. veronii* 2E, *P. veronii* 2E MUT and the reference strain *P. aeruginosa* PA01. ST was determined from culture supernatants supplemented with different carbon sources: hydrophilic glucose and hydrophobic sunflower oil.

Culture supernatants	Surface Tension (dyne/cm)
Culture medium (sunflower oil, glucose)	77.87
Pseudomonas aeruginosa PA01, glucose	35.31
Pseudomonas aeruginosa PA01, sunflower oil	38.93
Pseudomonas veronii 2E, glucose	76.22
Pseudomonas veronii 2E, sunflower oil	60.17
Pseudomonas veronii 2E MUT, sunflower oil	75.24

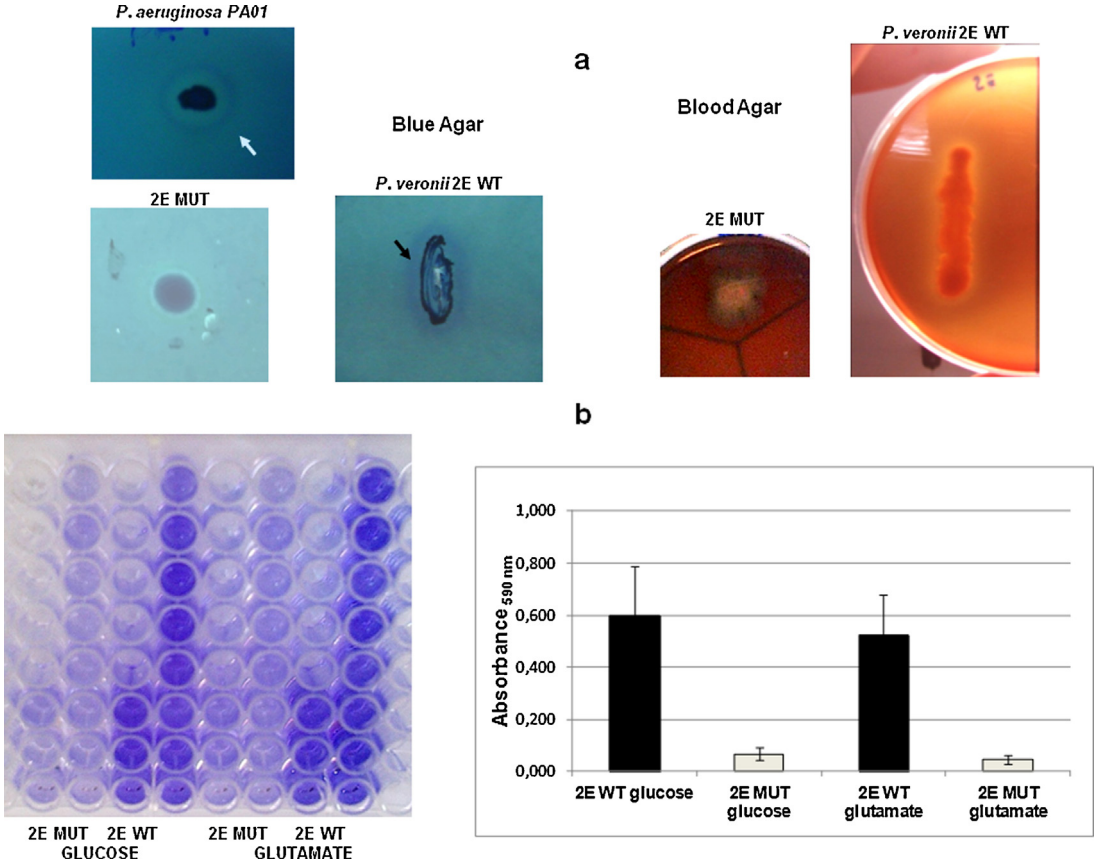

Fig. 3. (a) Biosurfactant production results in Blue Agar and Blood Agar tests. (b) Biofilm development by *P. veronii* 2E WT and the mutant 2E MUT, a deficient biosurfactant producer, evaluated by the rapid 96-well microtiter plate-CV technique.

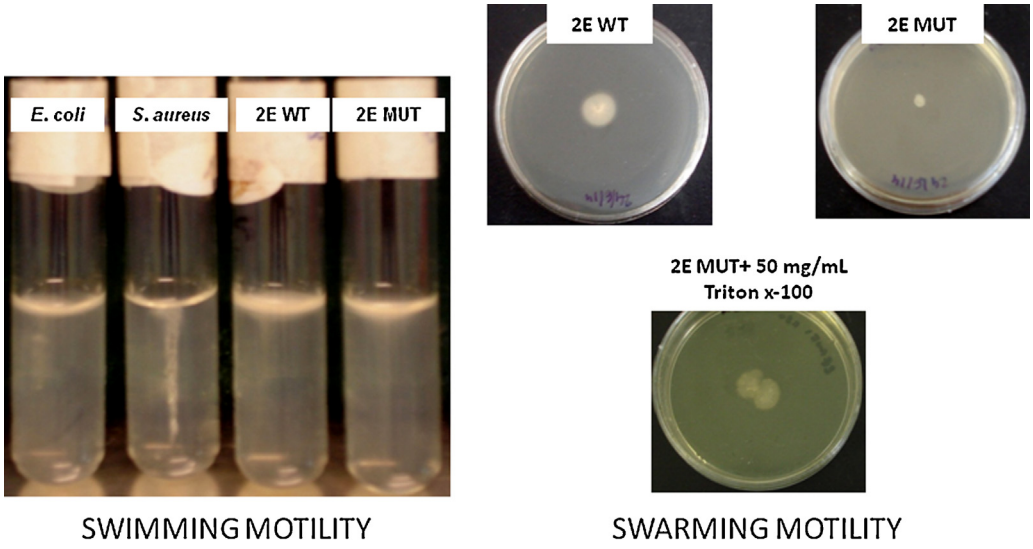

Fig. 4. Swimming and swarming motilities of *P. veronii* 2E WT and the mutant 2E MUT, a deficient biosurfactant producer.

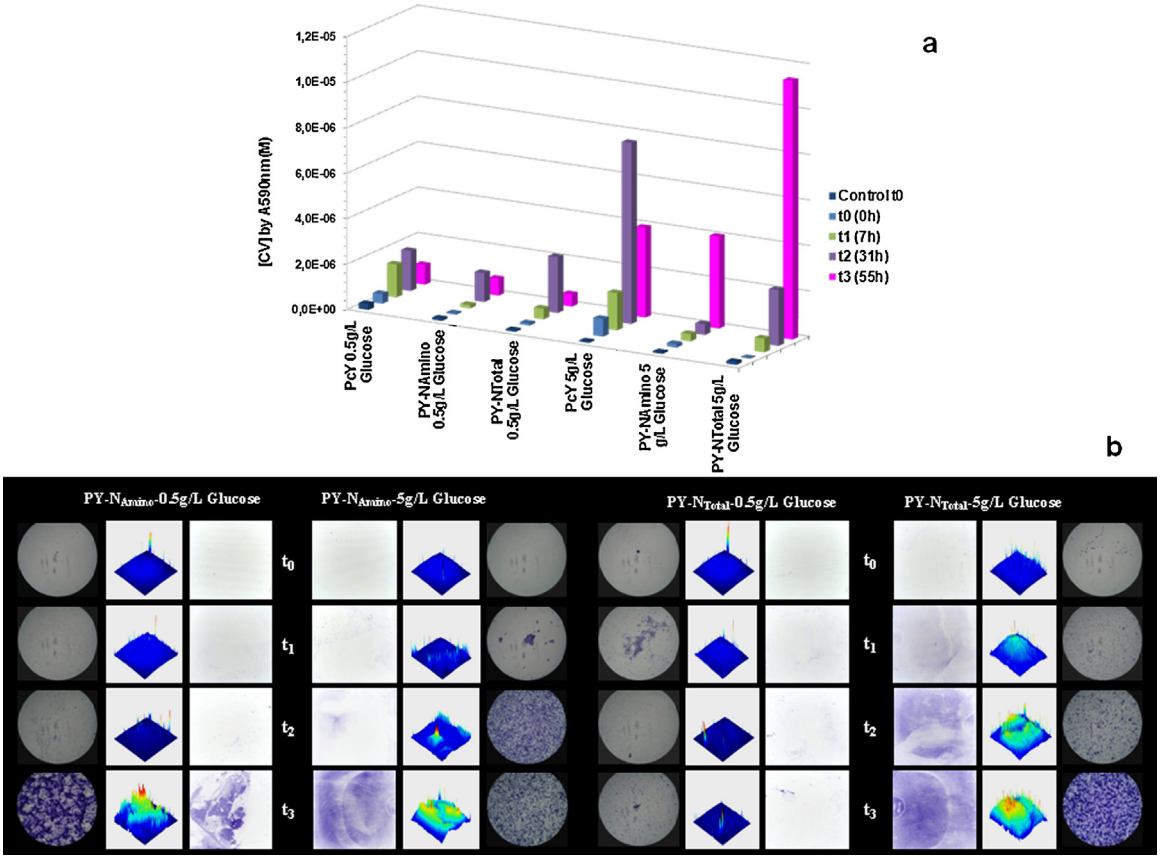

Fig. 5. Influence of organic nitrogen source (PcY, PY-glucose complex media) on biofilm development evaluated by two methods: (a) CV assay and (b) image capturing and 3D-pattern development (t_0 = 0 h, t_1 = 7 h, t_2 = 31 h and t_3 = 55 h).

synthesis. In fact, swarming motility was recovered when adding 50 mg/mL Triton X-100 to swarming agar (Fig. 4), confirming its dependence on the surfactant activity for this type of bacterial motility. In conclusion, the biosurfactant production and consequently cell motility are determinant factors on biofilm formation for *P. veronii* 2E.

3.2. Nitrogen source effect on biofilms

PY-Complex media were chosen based on the variation of N content and nature of the commercial protein hydrolysates: PcY contained casein peptone (12.7 w/w% Total Nitrogen, 3.7 w/w% NH_2- Nitrogen) while PY was formulated with meat peptone (14.0 w/w% Total Nitrogen, 2.6 w/w% NH_2-Nitrogen). PY-N_{Total} main-

tained the same meat peptone concentration as casein peptone in PcY (2.5 g/L), so the difference between them was the contribution of both Total Nitrogen and NH_2-Nitrogen to the medium. PY-N_{Amino} contained the same proportion of Total Nitrogen than PcY, but a lower proportion of NH_2-Nitrogen.

The results obtained with these complex media supplemented with 0.5 g/L or 5 g/L glucose are presented in Fig. 5. The same effect of carbon source concentration previously observed with PcY, was detected with PY-N_{Total} and PY-N_{Amino}. A slightly higher biofilm development was denoted with PcY-0.5 g/L glucose up to an incubation of 7 h, sampled before the medium renewal procedure, which was clearly evidenced by the CV method and the image capture (Fig. 2b and Fig. 5a and b). Using 5 g/L glucose, the best coverage was achieved with PY-N_{Total} at 55 h. Results of CV measurements (Fig. 5a) complemented with the images and 3D patterns (Fig. 5b) supported that the surface was totally colonized with an homogeneous biofilm characterized by the presence of bacterial aggregates.

Regarding nitrogen source, a comparison between organic-N (PY) and inorganic-N (M9) revealed that with the same glucose concentration (5 g/L) only a flat biofilm was developed with M9. Evidently for *P. veronii* 2E biofilm establishment yields, the best choice for a nitrogen source and its proportion would be compatible with the PY-N_{Total} complex medium. Once again, during the time of these experiments, no cell detachment was detected.

When planktonic growth was evaluated by measuring $OD_{600\,nm}$, the highest values ($OD_{600\,nm} = 1$) were obtained with M9 basal medium, independently of the carbon source. As expected, the maximal planktonic biomass correlated to the minimal attached biomass on the coverslip. Furthermore, the addition of fresh nutrient supply resulted in a selection of sessile cells when medium renewal was carried out at 30 h of incubation and planktonic cells were washed out. This separation between bacterial populations was beneficial for biofilm establishment, especially in PY-N_{Amino} basal medium (see Fig. 5b, t_2 and t_3).

3.3. Influence of Fe(II) on biofilm development

As studied by other authors in *Pseudomonas aeruginosa* [18–20], the presence of bioavailable Fe(II) may contribute to biofilm establishment. Thus, the influence of 3 μM Fe(II) addition to M9 or PY basal media was evaluated with 5 g/L and 0.5 g/L glucose respectively. These glucose concentrations were chosen in order to discriminate visible changes in biofilm using the implemented methology, for poor biofilm developments were observed as described above (Figs. 1 and 2). Fe(II) concentration (3 μM) was considered proper for this assay, taking into account the results reported by Glick et al. [21] and OíToole et al. [6] for *P. aeruginosa* and *Pseudomonas fluorescens* respectively, corresponding to the border line between limiting and non-limiting conditions.

A positive effect of the Fe(II) presence was clearly registered when M9 was used as basal medium (Fig. 6a and b). Comparing with M9 without Fe(II) (Fig. 1), a significant increase of biofilm development with time up to 55 h was confirmed by CV technique and image capturing, showing an homogeneous and denser carpet in the 3D surface patterns. Contrastingly, when PY media were used only a slight increase in biofilm formation at $t_1 = 7$ h with a consequent detachment at higher incubation times was registered (Fig. 6a and b). When a complex basal medium is supplemented with Fe(II), several interactions appeared between the cation and the organic compounds, which could be the explanation of the weak effect detected; the bioavailability was compromised. Fe(II) remained soluble and evidently bioavailable when added to M9.

According to the results in Fig. 6, following time evolution (t_1–t_3), the *P. veronii* 2E biofilm in presence of Fe(II) developed in thickness once the surface was totally covered. A more

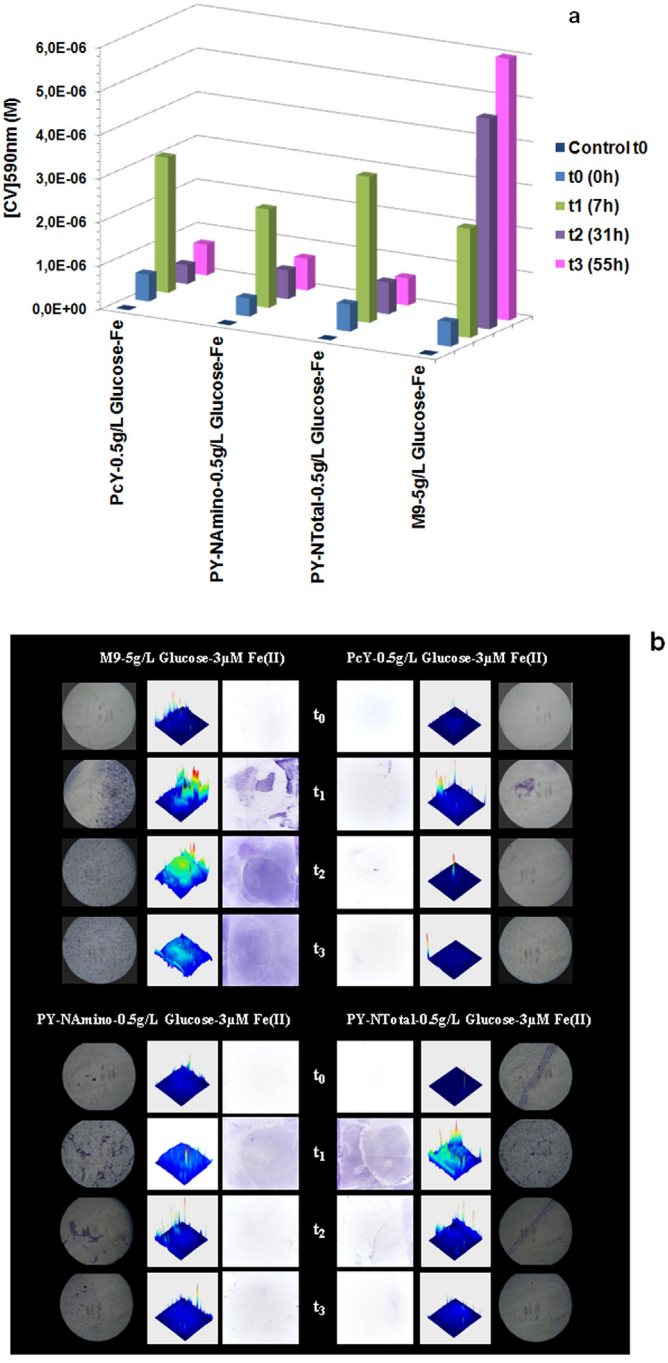

Fig. 6. Kinetics of biofilm development in different basal media with 3 μM Fe(II) evaluated by two methods: (a) CV assay and b. image capturing and 3D-pattern development ($t_0 = 0$ h, $t_1 = 7$ h, $t_2 = 31$ h and $t_3 = 55$ h).

structured biofilm was obtained under these experimental conditions, as reported by other *Pseudomonas*. As found by Glick et al. [21] Fe-limiting conditions would be the responsible of rhamnolipid synthesis and twitching motility stimulation leading to a flat biofilm for *P. aeruginosa*, in contrast with a structured biofilm obtained when Fe was present.

4. Conclusions

The complementation between three different techniques for studying biofilm development was extremely useful to avoid misinterpretations of the results. In this context, for *P. veronii* 2E, the

best attachment was achieved with a complex basal medium (PY) supplemented with 5 g/L glucose up to 55 h. Fe(II) influenced positively at any time only when M9 basal medium was used. In contrast with complex media, the Fe(II)-effect was clearly favorable only at short incubation times, accompanied by a fast detachment. This work allowed the determination of the optimal nutritional conditions for biofilm establishment over glass in static systems. This study was necessary to understand the *P. veronii* 2E adhesion to surfaces, which was not reported before. Regarding the limitations of these results in terms of their extrapolation to a bioreactor performance, they represent the basic and useful knowledge for the development of the next steps to be carried out: the proved metal-biosortive mechanisms applied to an adequate design of a proper biofilm-reactor for Cd(II)-Zn(II) removal with *P. veronii* 2E as biosorbent.

Acknowledgements

This work was supported by the Universidad Nacional de General Sarmiento, Agencia Nacional de Promoción Científica y Tecnológica (ANPCyT), PICTO N°36782 and PICTO N°00086 and Consejo Nacional de Investigaciones Científicas y Tecnológicas (CONICET).

We are grateful to Miss Leticia Rossi for the English language revision.

References

[1] R. Singh, P. Debarati, R.K. Jain, Biofilms: implications in bioremediation, Trends Microbiol. 14 (9) (2006) 389–397.
[2] B. Halan, K. Buehler, A. Schmid, Biofilms as living catalysis in continuous chemical syntheses, Trends Biotechnol. 30 (9) (2012) 453–465.
[3] J.D. Shrout, D.L. Chopp, C.L. Just, M. Hentzer, M. Givskov, M.R. Parsek, The impact of quorum sensing and swarming motility on *Pseudomonas aeruginosa* biofilm formation is nutritionally conditional, Mol. Microbiol. 62 (5) (2006) 1264–1277.
[4] K. Sauer, M.C. Cullen, A.H. Rickard, L.A.H. Zeef, D.G. Davies, P. Gilbert, Characterization of nutrient-induced dispersion in *Pseudomonas aeruginosa* PAO1, Biofilm J. Bacteriol. 186 (21) (2004) 7312–7326.
[5] J. Sheikh, S. Hicks, M. Dall'Agnol, A.D. Phillips, J.P. Nataro, Roles for Fis and YafK in biofilm formation by enteroaggregative *E. coli*, Mol. Microbiol. 41 (5) (2001) 983–997.
[6] G. OíToole, R. Kolter, Initiation of biofilm formation in *Pseudomonas fluorescens* WCS365 proceeds via multiple, convergent signalling pathways: a genetic analysis, Mol. Microbiol. 28 (3) (1998) 449–461.
[7] J.D. Mathias, P. Stoodley, Applying the digital image correlation method to estimate the mechanical properties of bacterial biofilms subjected to a wall shear stress, Biofouling 25 (8) (2009) 695–703.
[8] D.L. Vullo, H.M. Ceretti, M.A. Daniel, S.A.M. Ramírez, A. Zalts, Cadmium, zinc and copper biosorption mediated by *Pseudomonas veronii* 2E, Bioresour. Technol. 99 (2008) 5574–5581.
[9] N. Mendez, S.A.M. Ramirez, H.M. Ceretti, A. Zalts, R. Candal, D.L. Vullo, *Pseudomonas veronii* 2E surface interactions with Zn(II) and Cd(II), Global J. Environ. Sci. Technol. 1 (2011) 3.
[10] B. Jähne, Digital Image Processing, fifth ed., Springer-Verlag, Berlin, 2002.
[11] R.C. Gonzalez, R. Woods, S. Eddins, Digital Image Processing Using Matlab, Prentice Hall, London, 2004.
[12] R.S. Bivand, E.J. Pebesma, V. Gómez-Rubio, Applied Spatial Data Analysis with R, Springer, New York, 2008.
[13] J.C. Russ, The Image Processing Handbook, fifth ed., CRC Press, Boca Raton, 2006.
[14] K. Falconer, Fractal Geometry: Mathematical Foundations and Applications, Wiley, New York, 2003.
[15] M.R. Barrionuevo, D.L. Vullo, Bacterial swimming, swarming and chemotactic response to heavy metal presence: which could be the influence on wastewater biotreatment efficiency? World J. Microbiol. Biotechnol. 28 (2012) 2813–2825.
[16] M. Klausen, A. Heydorn, P. Ragas, L. Lambertsen, A. Aaes-Jørgensen, S. Molin, T. Tolker-Nielsen, Biofilm formation by *Pseudomonas aeruginosa* wild type, flagella and type IV pili mutants, Mol. Microbiol. 48 (6) (2003) 1511–1524.
[17] M.R. Barrionuevo, D.L. Vullo, Extracción y Caracterización Preliminar de Biosurfactantes Producidos por Bacterias Autóctonas de la Cuenca del Reconquista, in: M. dos Santos Afonso, R.M. Torres Sanchez (Eds.), Ciencia y Tecnología Ambiental: un enfoque integrador, Asociación Argentina para el Progreso de las Ciencias Buenos Aires-Argentina, 2012, pp. 701–706.
[18] Harmsen, L. Yang, S.J. Pamp, T. Tolker-Nielsen, An update on *Pseudomonas aeruginosa* biofilm formation tolerance, and dispersal, FEMS Inmunol. Med. Microbiol. 59 (2010) 253–268.
[19] G.M. Patriquin, E. Banin, C. Gilmour, R. Tuchman, E.P. Greenberg, K. Poole, Influence of quorum sensing and iron on twitching motility and biofilm formation in *Pseudomonas aeruginosa*, J. Bacteriol. 190 (2) (2008) 662–671.
[20] E. Banin, M.L. Vasil, E.P. Greenberg, Iron and *Pseudomonas aeruginosa* biofilm formation, PNAS 102 (31) (2005) 11076–11081.
[21] R. Glick, C. Gilmour, J. Tremblay, S. Satanower, O. Avidan, E. Déziel, E.P. Greenberg, K. Poole, E. Banin, Increase in rhamnolipid synthesis under iron-limiting conditions influences surface motility and biofilm formation in *Pseudomonas aeruginosa*, J. Bacteriol. 192 (12) (2010) 2973–2980.